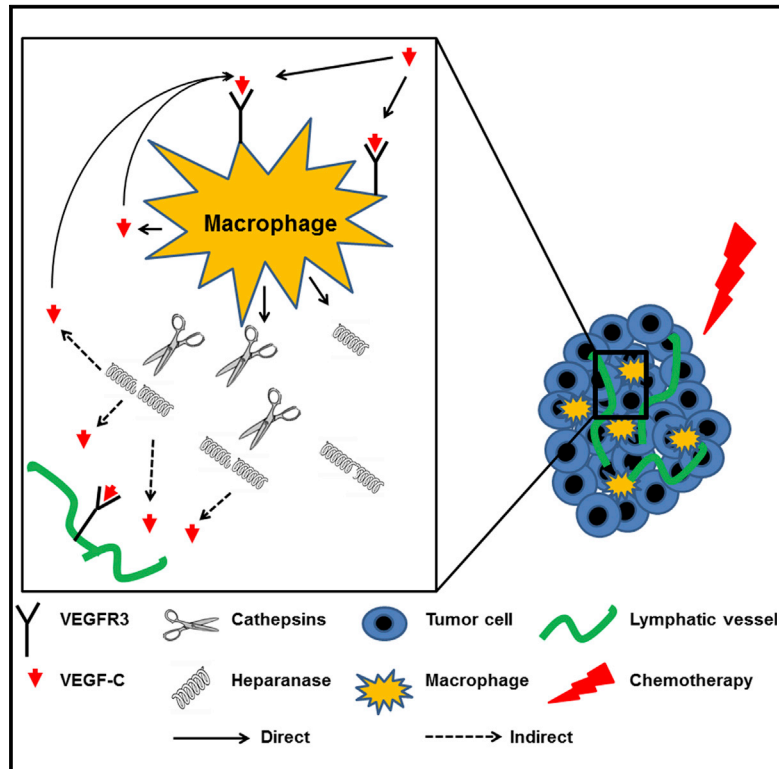


Macrophage-Induced Lymphangiogenesis and Metastasis following Paclitaxel Chemotherapy Is Regulated by VEGFR3

Graphical Abstract



Authors

Dror Alishekevitz,
Svetlana Gingis-Velitski,
Orit Kaidar-Person, ...,
Jonathan P. Sleeman, Israel Vlodavsky,
Yuval Shaked

Correspondence

yshaked@tx.technion.ac.il

In Brief

Alishekevitz et al. now find that macrophages expressing VEGFR3 home in large numbers to chemotherapy-treated tumors. At the treated tumor site, macrophages promote lymphangiogenesis and subsequent metastasis via the VEGF-C/VEGFR3 axis. Blocking VEGFR3 in treated tumors hinders metastasis through the inhibition of pro-metastatic macrophage activity.

Highlights

- Chemotherapy promotes macrophage colonization of tumors
- Macrophages induce lymphangiogenesis in chemotherapy-treated tumors
- Macrophages secrete cathepsins, VEGF-C, and heparanase in a VEGFR3-dependent manner
- Blocking VEGFR3 in macrophages inhibits lymphangiogenesis and subsequent metastasis



Macrophage-Induced Lymphangiogenesis and Metastasis following Paclitaxel Chemotherapy Is Regulated by VEGFR3

Dror Alishekevitz,¹ Svetlana Gingis-Velitski,¹ Orit Kaidar-Person,² Lilach Gutter-Kapon,¹ Sandra D. Scherer,^{3,4} Ziv Raviv,¹ Emmanuelle Merquiol,⁵ Yael Ben-Nun,⁵ Valeria Miller,¹ Chen Rachman-Tzemah,¹ Michael Timaner,¹ Yelena Mumblat,¹ Neta Ilan,¹ David Loven,⁶ Dov Hershkovitz,⁷ Ronit Satchi-Fainaro,⁸ Galia Blum,⁵ Jonathan P. Sleeman,^{3,4} Israel Vlodavsky,¹ and Yuval Shaked^{1,9,*}

¹Department of Cell Biology and Cancer Science, Rappaport Faculty of Medicine, Technion – Israel Institute of Technology, 3109601 Haifa, Israel

²Division of Oncology, Rambam Health Care Campus, 3109601 Haifa, Israel

³Institute of Toxicology and Genetics, Karlsruhe Institute of Technology (KIT), 76344 Eggenstein-Leopoldshafen, Germany

⁴Centre for Biomedicine and Medical Technology Mannheim (CBTM), Medical Faculty Mannheim of the University of Heidelberg, 68167 Mannheim, Germany

⁵The School of Pharmacy, Faculty of Medicine, The Hebrew University of Jerusalem, 9112001 Jerusalem, Israel

⁶Department of Oncology, Ha'Emek Medical Center, 1834111 Afula, Israel

⁷Department of Pathology, Rambam Health Care Campus, 3109601 Haifa, Israel

⁸Department of Pharmacology, Faculty of Medicine, Tel Aviv University, 6997801 Tel Aviv, Israel

⁹Lead Contact

*Correspondence: yshaked@tx.technion.ac.il

<http://dx.doi.org/10.1016/j.celrep.2016.09.083>

SUMMARY

While chemotherapy strongly restricts or reverses tumor growth, the response of host tissue to therapy can counteract its anti-tumor activity by promoting tumor re-growth and/or metastases, thus limiting therapeutic efficacy. Here, we show that vascular endothelial growth factor receptor 3 (VEGFR3)-expressing macrophages infiltrating chemotherapy-treated tumors play a significant role in metastasis. They do so in part by inducing lymphangiogenesis as a result of cathepsin release, leading to VEGF-C upregulation by heparanase. We found that macrophages from chemotherapy-treated mice are sufficient to trigger lymphatic vessel activity and structure in naive tumors in a VEGFR3-dependent manner. Blocking VEGF-C/VEGFR3 axis inhibits the activity of chemotherapy-educated macrophages, leading to reduced lymphangiogenesis in treated tumors. Overall, our results suggest that disrupting the VEGF-C/VEGFR3 axis not only directly inhibits lymphangiogenesis but also blocks the pro-metastatic activity of macrophages in chemotherapy-treated mice.

INTRODUCTION

One of the most challenging obstacles and leading cause of death in breast cancer patients is the outburst of metastatic disease that may occur years after the removal of the primary

tumor. Lymph node involvement at time of diagnosis in the absence of distant metastatic disease (i.e., locally advanced diseases) significantly reduces survival rate (Fisher et al., 1983). The lymphatic system serves as a major route for tumor cells disseminating from the primary tumor site. Disseminated tumor cells can be transported to the regional lymph node, where they can either lodge and metastasize or metastasize through the lymph nodes to remote areas (Stacker et al., 2002). Vascular endothelial growth factor receptor (VEGFR) 3 is the key receptor that regulates lymphangiogenesis. It can bind both VEGF-C and VEGF-D (Sleeman and Thiele, 2009). The expression of VEGF-C by tumors, in particular, correlates with poor prognosis for a wide variety of cancers, in part due to an increase in lymphangiogenesis (Alitalo and Detmar, 2012). Increased VEGF-C levels induce intra-tumoral lymphangiogenesis, resulting in significantly enhanced metastasis to regional lymph nodes and to lungs (Skobe et al., 2001). As a consequence, the combined neutralization of VEGF-C and VEGF-D by soluble VEGFR3 resulted in a complete abolishment of lymphangiogenesis (Mäkinen et al., 2001).

Besides the cytotoxic effect of chemotherapy that ultimately kills proliferating tumor cells, it has been recently reported that chemotherapy can induce several host effects that can facilitate tumor growth and metastasis, thereby limiting the anti-tumor activity of the drug (for review, see Shaked, 2016). Mice treated with paclitaxel (PTX) succumb to breast cancer metastasis earlier than mice treated with vehicle control in a pulmonary metastatic model. The secretion of matrix metalloproteinase 9 (MMP9) by bone-marrow-derived cells (BMDCs) colonizing treated tumors is a possible inducer of the metastatic process (Gingis-Velitski et al., 2011). In addition, myeloid

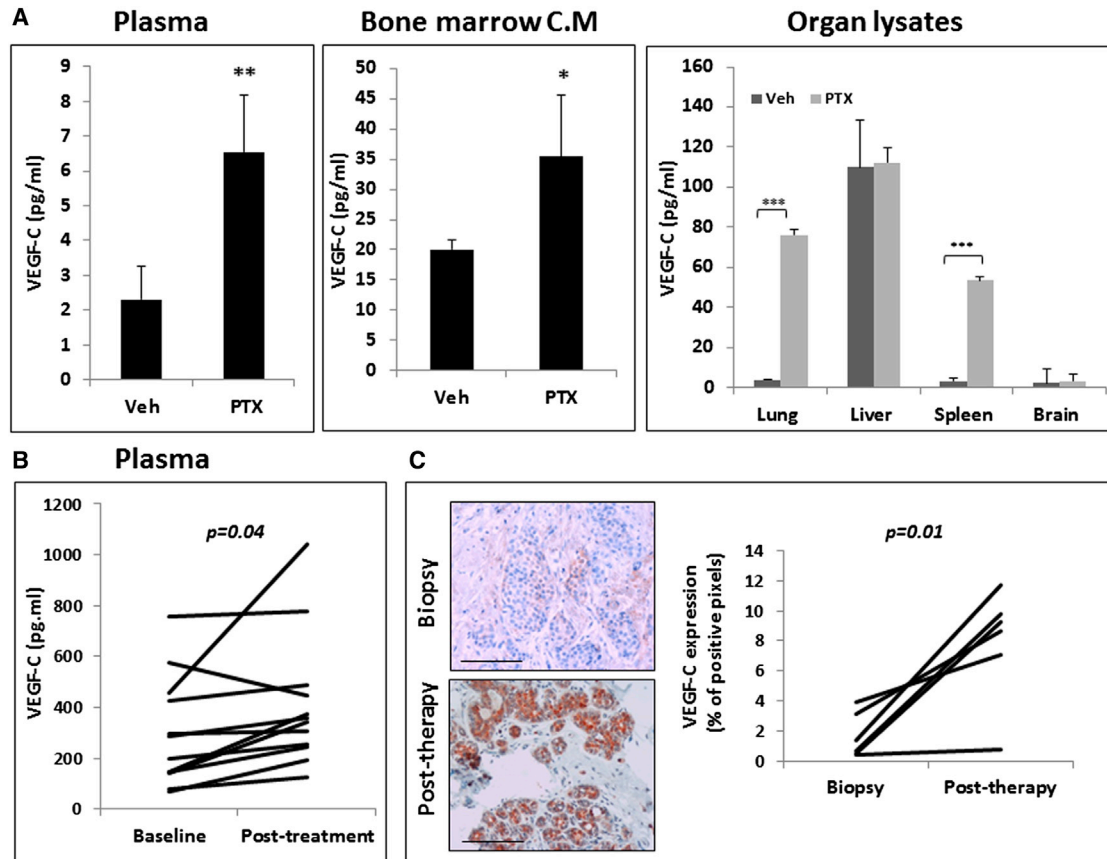


Figure 1. VEGF-C Is Elevated in Plasma and Tissue following Paclitaxel Chemotherapy

(A) Non-tumor-bearing BALB/c mice ($n = 5/\text{group}$) were treated with 25 mg/kg PTX or vehicle control (Veh). After 24 hr, blood was drawn and plasma was separated. Bone marrow was flushed from the femurs, and cells were grown in culture from which conditioned medium (CM) was collected. Lungs, liver, spleen, and brain were harvested and lysates were prepared. Levels of VEGF-C were evaluated in all specimens using ELISA.

(B) Blood was drawn from breast carcinoma patients ($n = 12$) at baseline and 24 hr after the first treatment with PTX. Plasma was evaluated for VEGF-C levels.

(C) Breast tumor specimens obtained from patients before (baseline) and after chemotherapy were stained for VEGF-C (red). Scale bar, 100 μm . The percentage of positive pixels was determined and plotted ($n = 6$ sample pairs). Error bars indicate SD. * $p < 0.05$; ** $0.01 \geq p > 0.001$; *** $p \leq 0.001$ (two-tailed Student's *t* test).

cells and macrophages have also been shown to contribute to tumor re-growth by promoting drug resistance. For example, Shree et al. demonstrated that macrophages from PTX-treated mice contribute to breast cancer resistance to therapy via the secretion of cathepsins (Shree et al., 2011). Others demonstrated that following anti-cancer therapies, macrophages limit the anti-tumor efficacy of the therapy sometimes through unknown mechanisms (Timaner et al., 2015; Welford et al., 2011). Thus, these collective studies suggest that host cells, in response to therapy, generate pro-metastatic and pro-tumorigenic effects that promote tumor regrowth, metastasis, and resistance to therapy.

In the current study we investigated the role of the VEGF-C/VEGFR3 axis in tumor spread following PTX chemotherapy. We found that VEGFR3 expressed by chemotherapy-activated macrophages contributes to lymphangiogenesis largely by promoting the secretion of cathepsins, leading to increased heparanase activity. This, in turn, induces the expression of VEGF-C, ultimately leading to lymphangiogenesis and subsequently metastasis.

RESULTS

Paclitaxel Induces VEGF-C Expression

Our previous studies indicate that chemotherapy administered at conventional doses increases the levels of several circulating growth factors (Shaked et al., 2008; Shaked et al., 2009). We used a protein array to analyze plasma from non-tumor bearing BALB/c mice 24 hr after the administration of PTX chemotherapy. VEGF-C levels were substantially increased in the plasma of PTX-treated mice in comparison to control mice (data not shown). In light of the known role of VEGF-C in tumor lymphangiogenesis and metastasis (Mandriota et al., 2001; Skobe et al., 2001), we further investigated its expression and functional role in response to chemotherapy. We found a significant increase in the levels of VEGF-C in plasma, lungs, and spleen, as well as conditioned medium of BMDCs of PTX-treated mice in comparison to vehicle-treated mice (Figure 1A). Similarly, VEGF-C levels were elevated in the plasma of breast cancer patients ($n = 12$) 24 hr after PTX treatment when compared to baseline levels (Figure 1B). Furthermore, tissue derived from tumors

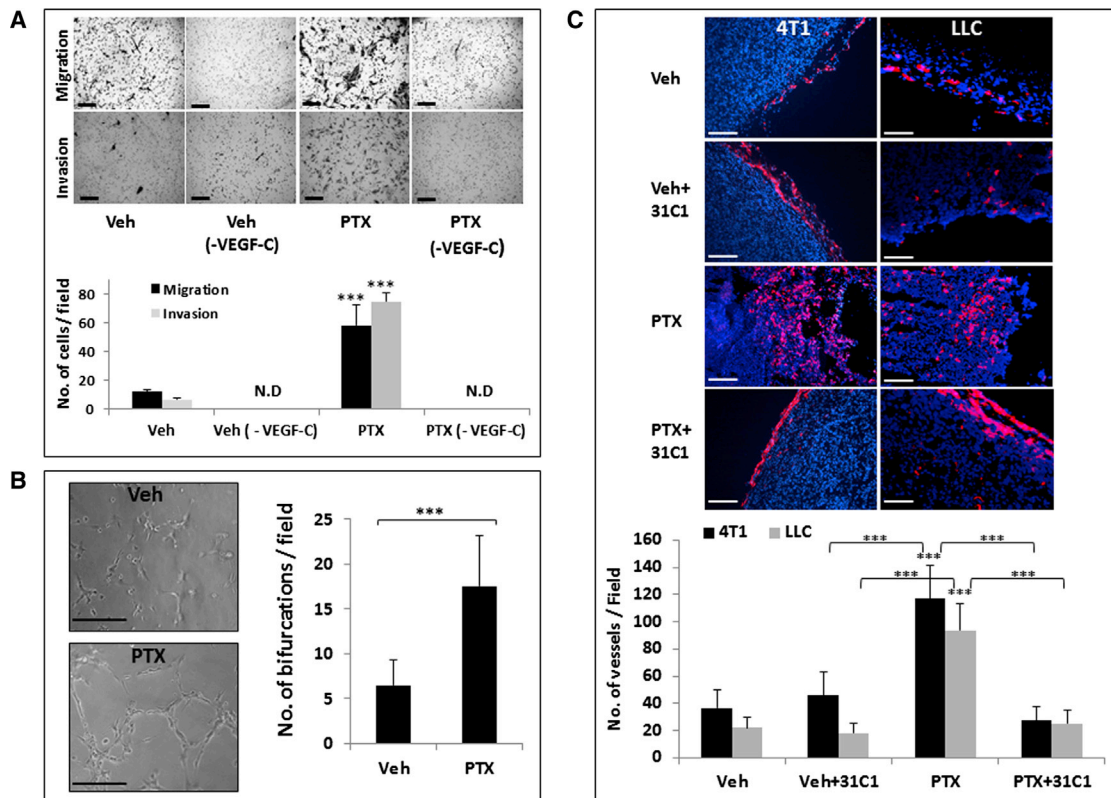


Figure 2. Elevation in Lymphatic Endothelial Cell Activity following Paclitaxel Therapy

(A and B) Plasma was drawn from non-tumor-bearing BALB/c mice 24 hr after they were treated with vehicle (Veh) or PTX (n = 3 mice/group). Half the plasma from Veh- or PTX-treated mice was depleted of VEGF-C by immunoprecipitation with neutralizing anti-VEGF-C antibodies. (A) Migration and invasion of lymphatic endothelial cells (LECs) were tested in the presence of the plasma samples using the Boyden chamber assay as described in [Experimental Procedures](#). The number of invading and migrating cells per field was counted and plotted (n = 15/group). (B) LECs were seeded onto Matrigel-coated plates and cultured for 24 hr in growth medium supplemented with 10% plasma from vehicle- or PTX-treated mice. Tube formation was assessed. Representative phase contrast images are shown. The number of bifurcations was counted (n = 12 fields/group). Scale bar, 200 μ m. N.D., non-detectable. (C) 4T1 and LLC cells were implanted in BALB/c and C57Bl/6 mice, respectively (n = 5/group). When tumors reached a size of 500 mm³, treatment with vehicle, PTX, anti-VEGFR3 antibodies (31C1), or the combination of PTX and 31C1 was initiated. After 3 days, tumors were harvested and sections were prepared and stained for LYVE-1, a LEC marker (red). DAPI was used to stain nuclei (blue). Scale bar, 200 μ m. The number of lymphatic vessels in the tumors was counted per field (n = 20/group). Error bars indicate SD. ***p \leq 0.001 (one-way ANOVA followed by Tukey's post hoc test).

of chemotherapy-treated breast cancer patients exhibited significantly increased VEGF-C expression in comparison to baseline biopsy specimens extracted before treatment with chemotherapy (n = 6) (Figure 1C). Of note, treatment with FOLFOX and gemcitabine, but not cisplatin chemotherapy, increased VEGF-C levels in the plasma, lungs, and conditioned medium of BMDCs of non-tumor-bearing mice (Figure S1). Overall, these results demonstrate that acute administration of certain chemotherapy drugs such as PTX induces a significant increase in VEGF-C levels in tumors, plasma, and various organs

Paclitaxel-Induced VEGF-C Expression Promotes Lymphatic Endothelial Cell Activity In Vitro and In Vivo

To determine whether the induction in VEGF-C levels in the plasma of PTX-treated mice alters lymphatic endothelial cell (LEC) activity, we tested LEC migration, invasion, and tube formation in the presence of plasma from control or PTX-treated mice. All three processes were enhanced in the presence of plasma from PTX-treated mice compared to plasma from vehicle

control mice. Notably, when VEGF-C was depleted from plasma of PTX-treated mice by immunoprecipitation, the enhancement of LEC invasion and migration was completely abolished, suggesting that PTX-induced LEC activity is primarily regulated by VEGF-C (Figures 2A and 2B).

VEGFR3 is the major receptor for VEGF-C-induced lymphangiogenesis (Kukk et al., 1996). We therefore assessed lymphangiogenesis in tumors of PTX-treated mice in the presence of VEGFR3-specific antibodies (31C1) that block receptor function (Matsumoto et al., 2013). To this end, 4T1 and Lewis lung carcinoma (LLC) tumors implanted in mice were allowed to grow until they reached 500 mm³, at which point treatment with PTX and/or 31C1 was initiated. After 3 days, tumors were removed and tumor sections were stained with LYVE-1 antibody for the detection of lymphatic vessels. In control and 31C1-treated mice, lymphatic vessels were localized to the periphery of the tumors. In contrast, in PTX-treated mice, lymphatic vessels were found both at the periphery and in the tumor center, and their number was significantly increased. This effect was reversed in mice

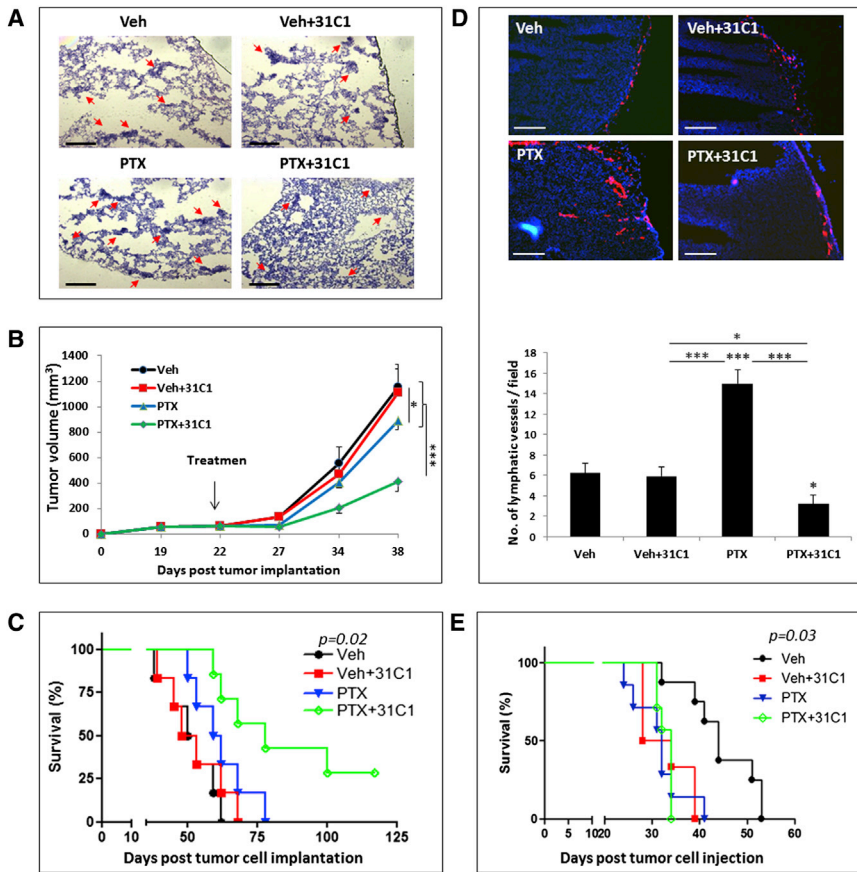


Figure 3. Tumor Growth and Metastasis in Mice Treated with Paclitaxel and/or 31C1

(A) 8- to 10-week-old female BALB/c mice ($n = 5/\text{group}$) were orthotopically implanted with 4T1 cells into the mammary fat pad (0.5×10^6). When tumors reached a size of 300 mm^3 , treatment with vehicle, PTX, 31C1, or a combination of the two drugs was initiated. When tumors reached endpoint ($\sim 1,000 \text{ mm}^3$), mice were sacrificed. Lungs were removed and lung sections were stained with H&E and assessed for metastasis. Metastatic lesions per magnified field were counted ($n = 15 \text{ fields}/\text{group}$). Red arrows point at micrometastases. Scale bar, $200 \mu\text{m}$.

(B) LM2-4 human breast carcinoma cells (2×10^6) were implanted into the mammary fat pad of 8- to 10-week-old female CB.17 SCID mice ($n = 5/\text{group}$). When tumors reached $100\text{--}150 \text{ mm}^3$, treatment with PTX and/or 31C1 was initiated. Primary tumor growth was measured and plotted.

(C) In a parallel experiment, 3 days after PTX therapy, tumors were resected and mouse survival was monitored ($n = 6\text{--}7 \text{ mice}/\text{group}$). A Kaplan-Meier survival curve was plotted.

(D) The resected primary tumors (from C) were stained for LYVE-1 (red). DAPI was used to stain nuclei (blue). Scale bar, $200 \mu\text{m}$. The number of lymphatic vessels in the tumors was counted per field ($n = 20/\text{group}$).

(E) Vehicle (Veh), PTX, 31C1, or a combination of the two drugs was administered to BALB/c mice. After 24 hr, mice were injected with 25×10^4 4T1 cells through the tail vein to generate pulmonary experimental metastasis. Mouse survival was monitored and a Kaplan-Meier survival curve was plotted ($n = 7\text{--}8 \text{ mice}/\text{group}$). Error bars indicate SD. * $p < 0.05$; *** $p \leq 0.001$ (one-way ANOVA followed by Tukey's post hoc test).

treated with a combination of PTX and 31C1 (PTX+31C1). Of note, the single dose of 31C1 monotherapy had a negligible anti-lymphangiogenesis effect at this time point (Figure 2C). Taken together, the in vitro and in vivo results suggest that PTX promotes lymphangiogenesis throughout the VEGF-C/VEGFR3 axis, in part via host effects.

Blocking the VEGF-C/VEGFR3 Pathway in Mice Treated with PTX Inhibits Primary Tumor Growth and Metastasis

We next asked whether the blockade of the VEGF-C/VEGFR3 pathway following PTX therapy inhibits tumor cell dissemination from the primary tumor and its colonization at metastatic sites. To test tumor cell dissemination, 4T1 cells implanted into the mammary fat pad of BALB/c mice were allowed to grow until they reached 300 mm^3 , at which point, treatment with PTX and/or 31C1 was initiated. At end point for each group, lungs were removed and assessed for micrometastases. Mice treated with PTX exhibited a significant increase in the number of metastatic lesions when compared to control mice. This effect was reversed in mice treated with a combination PTX and 31C1 (Figures 3A and S2).

We next performed similar experiments using the metastatic LM2-4 cell line. LM2-4 cells were implanted into the mammary fat pad of severe combined immunodeficiency (SCID) mice.

When tumors reached $100\text{--}150 \text{ mm}^3$, treatment with PTX and/or 31C1 was initiated. Primary tumor growth of mice treated with PTX and 31C1 was significantly delayed compared to all other treatment groups (Figure 3B). Furthermore, mouse survival was significantly increased when the primary tumors were resected 3 days after PTX and/or 31C1 therapy (Figure 3C). In addition, the tumors in control, 31C1, and PTX+31C1 treatment groups exhibited a peripheral lymphatic vessel phenotype, in contrast to tumors from the PTX monotherapy group in which lymphatic vessels were both peripherally and centrally distributed (Figures 3D and S2B). These results are comparable to those shown in Figure 2C. In a parallel experiment, when the control group reached endpoint, lungs from all groups were removed and evaluated for metastatic lesions. Control mice exhibited an increased number of lesions in comparison to PTX- or PTX+31C1-treated groups (Figure S2C). Primary tumor growth and lymphatic vessel phenotypes were comparable in the A549 human lung carcinoma model (Figures S2D and S2E). Of note, tumor growth and the lymphatic vessel phenotype in tumors from mice treated with isotype control antibody was similar to that in vehicle control mice (Figure S2F; data not shown).

To test whether blocking the VEGF-C/VEGFR3 axis affects tumor cell seeding in the lungs, we used an experimental lung metastasis assay. BALB/c mice were treated with PTX and/or

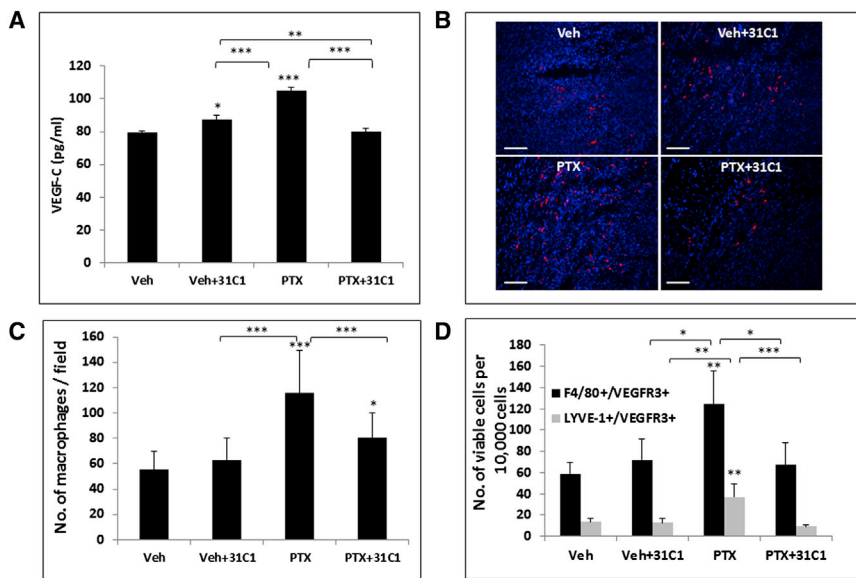


Figure 4. VEGF-C and VEGFR3 Expression in Macrophages from Paclitaxel- and/or 31C1-Treated Mice

(A) Peritoneal macrophages were harvested from non-tumor-bearing mice ($n = 4/\text{group}$) treated with vehicle (Veh), PTX, 31C1, or a combination of the two drugs and grown in culture. The level of VEGF-C in the conditioned medium was assessed by ELISA.

(B–D) 4T1 tumors were grown in BALB/c mice ($n = 4/\text{group}$) until they reached 500 mm^3 , at which point mice were treated with vehicle (Veh), PTX, 31C1, or a combination of the two drugs. After 3 days, tumors were harvested and tumor sections were stained with F4/80 (a specific macrophage marker, red), DAPI was used to stain nuclei (blue). Scale bar, $200 \mu\text{m}$ (B). The number of F4/80-positive cells per field was counted in the tumors ($n = 15$ fields/group) (C). In a parallel experiment, the harvested tumors ($n = 4/\text{group}$) were prepared as single-cell suspensions, stained (for VEGFR3, F4/80, and LYVE-1), and analyzed by flow cytometry. The number of tumor-associated, viable VEGFR3-expressing macrophages and viable

VEGFR3-expressing lymphatic endothelial cells was calculated based on the percentage of $\text{F4/80}^+/\text{VEGFR3}^+/\text{7AAD}^-$ or $\text{LYVE-1}^+/\text{VEGFR3}^+/\text{7AAD}^-$ cells, respectively, per 10,000 cells (D). Error bars indicate SD.

* $p < 0.05$; ** $0.01 \geq p > 0.001$; *** $p \leq 0.001$ (one-way ANOVA followed by Tukey's post hoc test).

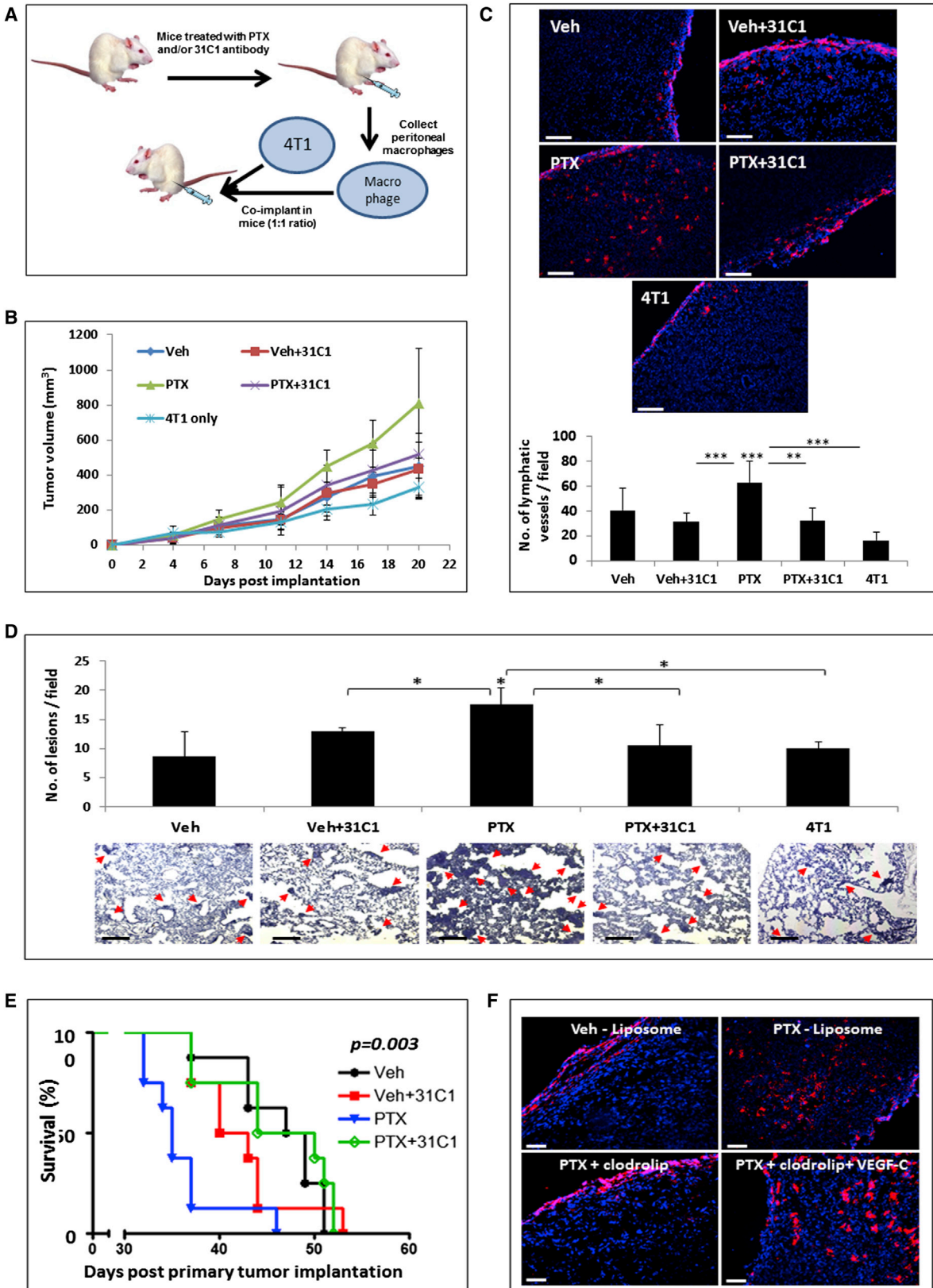
31C1. After 24 hr, the mice were injected with 4T1 cells via the tail vein, and survival was monitored. The results show that mice primed with PTX succumbed to metastasis earlier than control mice (Figure 3E), in line with a previous study (Gingis-Velitski et al., 2011). However, mice treated with 31C1 alone or a combination of PTX+31C1 exhibited seeding properties similar to PTX-treated mice. Taken together, these results suggest that the VEGF-C/VEGFR3 axis inhibits tumor cell dissemination from the primary tumor but does not affect seeding in PTX-treated mice. Importantly, the therapeutic benefit of the combination therapy of PTX and 31C1 was greater than PTX monotherapy in both primary tumor and metastatic disease models.

Upregulation of VEGF-C by Macrophages Contributes to Lymphangiogenesis in PTX-Treated Tumors

We next asked whether macrophages play a role in chemotherapy-induced metastasis through the VEGF-C/VEGFR3 pathway. To this end, peritoneal macrophages were extracted from non-tumor-bearing mice, and after 48 hr in culture, the level of VEGF-C in the conditioned medium was evaluated. VEGF-C levels were significantly increased in the conditioned medium of macrophages from PTX-treated mice compared to all other treatment groups. This effect was reversed in conditioned medium of macrophages obtained from mice treated with PTX+31C1. Of note, a slight but significant increase in VEGF-C levels was also observed in macrophages from mice treated with 31C1, an effect that was completely blocked when mice were treated with PTX+31C1, for reasons that are not clear (Figure 4A). Furthermore, no differences in VEGF-C levels were observed in a parallel in vitro experiment in which PTX and/or 31C1 were added directly to macrophage cultures, suggesting that the minimal increase in VEGF-C following PTX therapy is not related to the direct cytotoxic effect of the drugs (Figure S3A).

When focusing on VEGFR3, we found that a portion of peritoneal macrophages express VEGFR3, in line with a previous study (Zhang et al., 2014) (Figure S3B). However, the VEGFR3 expression levels were not affected in peritoneal macrophages from mice treated with PTX and/or 31C1 (Figure S3C). Although peritoneal macrophages have been extensively studied in the context of cancer, they are not “true” tumor-associated macrophages (Hagemann et al., 2009). We therefore evaluated the level of VEGFR3-expressing macrophages in treated tumors. We found that the number of macrophages infiltrating 4T1 tumors 3 days after PTX therapy was substantially and significantly increased compared to the PTX+31C1 group (Figures 4B and 4C). Importantly, the percentages of viable VEGFR3-expressing macrophages and lymphatic endothelial cells, isolated from mice bearing A549 tumors (from Figure S2D) treated with PTX and/or 31C1, were significantly higher in mice treated with PTX than in all other groups (Figures 4D and S3D). These results suggest that macrophages expressing VEGFR3 infiltrate tumors in response to PTX therapy.

To further test the effect of macrophages on PTX-dependent metastasis and lymphangiogenesis, we performed a co-implantation experiment using tumor cells and macrophages. Peritoneal macrophages obtained from non-tumor-bearing BALB/c mice treated with PTX and/or 31C1 were co-implanted with 4T1 tumor cells in a 1:1 ratio into the mammary fat pad of naive mice (Figure 5A). Tumor growth was monitored over time. Mice co-implanted with macrophages from PTX-treated mice exhibited a trend towards larger tumors when compared to those co-implanted with macrophages from control mice or from mice treated with PTX+31C1, although these results did not reach statistical significance (Figure 5B). At endpoint of the control group, primary tumors and lungs were removed and further assessed for lymphangiogenesis and metastasis, respectively.



(legend on next page)

Similar to the results shown in Figure 2C, the number of tumor lymphatic vessels (stained for LYVE-1 and podoplanin) was significantly higher in mice co-implanted with macrophages from PTX-treated mice than in control or combination-treated mice. These vessels were localized at the center of the tumor, whereas tumors of mice co-implanted with macrophages from control or combination-treated mice exhibited a peripheral lymphatic vessel distribution (Figures 5C and S4A). Furthermore, more metastases were observed in the lungs of mice co-implanted with macrophages from PTX-treated mice than in mice co-implanted with macrophages from the control or PTX+31C1-treated group (Figure 5D). However, implantation of macrophages from mice treated with VEGFR1 or VEGFR2 blocking antibodies (MF1 and DC101, respectively) in the presence of PTX did not restore lymphatic vessel distribution to the periphery. The PTX+DC101 group exhibited an intermediate peripheral lymphatic vessel phenotype (Figure S4B), suggesting that the effect is mostly specific to the VEGFR3 pathway. In addition, a significant increase in mortality was observed in mice co-implanted with 4T1 cells and macrophages from PTX-treated mice when compared to mice co-implanted with 4T1 cells and control macrophages or macrophages from PTX+31C1-treated mice (Figure 5E). Notably, no significant difference in endothelial microvessel density was observed among all treatment groups at the time point tested, ruling out the possibility that increased metastasis is associated with angiogenesis in our model (Figure S4C).

Next, we asked whether the link between macrophages and the lymphangiogenesis phenotype following PTX therapy is direct. To this end, we implanted BALB/c mice with 4T1 tumors and when tumors reached a size of 350 mm³, macrophages were depleted, using clodronate-containing liposomes (clodrolip). Macrophage depletion was verified in the spleens of clodrolip-treated mice (Figure S4D). After 72 hr, mice were treated with PTX with or without recombinant VEGF-C administered at a dose of 50 µg/mouse per day for 3 sequential days. Sequential VEGF-C administration was necessary in order to maintain increased VEGF-C levels in the circulation due to its short half-life (Veikkola et al., 2001). Tumors were removed on day 4 following PTX treatment and examined for lymphatic vessels. Macrophage-depleted mice treated with PTX and control mice exhibited similar numbers of peripherally distributed lymphatic vessels, in contrast to PTX-treated mice, in which lymphatic vessels were significantly greater in number and distributed centrally

within the tumor. When macrophage-depleted, PTX-treated mice were also injected with recombinant VEGF-C, the lymphatic vessel distribution and number were restored to that of PTX-treated mice (Figures 5F and S4E). In addition, levels of plasma VEGF-C were assessed in non-tumor-bearing BALB/c mice 72 hr after they were depleted of macrophages and 24 hr after they were treated with PTX. VEGF-C plasma levels were not significantly different from controls in mice depleted of macrophages regardless of PTX therapy (Figure S4F). Taken together, these results indicate that the lymphangiogenesis phenotype in tumors from mice treated with PTX is primarily regulated by macrophages, an effect that can be completely abolished by blocking VEGFR3 specifically on macrophages.

Macrophages Enhance Heparanase Activity via Cathepsins in a VEGFR3-Dependent Manner in Response to Paclitaxel

Previous studies indicate that heparanase upregulates VEGF-C expression, thus promoting metastasis via the lymphatic system (Cohen-Kaplan et al., 2008). We therefore assessed heparanase activity in peritoneal macrophages collected from mice treated with PTX and/or 31C1. The level of endogenous heparanase activity was ~2-fold higher in conditioned medium of macrophages from mice treated with PTX or PTX+31C1 than in control mice (Figure 6A). Notably, heparanase enzymatic activity was ~5-fold higher following exogenous addition of the 65-kDa latent enzyme to the conditioned medium of macrophages from mice treated with PTX relative to the control group, an effect that was blocked in the PTX+31C1-treated group (Figure 6B). Thus, blocking VEGFR3 inhibits the activation of exogenous latent heparanase, but not the endogenous enzyme, in macrophages from PTX-treated mice.

Macrophages secrete cathepsins in response to PTX (Shree et al., 2011). Since cathepsins cleave pro-heparanase into its active form (Arvatz et al., 2011), and heparanase upregulates VEGF-C expression (Cohen-Kaplan et al., 2008), we next asked whether PTX-induced cathepsin release from macrophages indeed contributes to the high VEGF-C expression in tumors. To this end, conditioned medium of peritoneal macrophages from PTX or PTX+31C1-treated mice was evaluated for its ability to activate exogenous latent heparanase in the presence or absence of cathepsin inhibitor. The results show that blockade of cathepsins inhibited the activation of exogenous latent heparanase incubated with conditioned medium of macrophages from

Figure 5. Macrophages from Mice Treated with Paclitaxel Promote Lymphangiogenesis in Therapy-Naive Tumors

(A–D) Peritoneal macrophages obtained from mice treated with vehicle (Veh), PTX, 31C1, or a combination of the two drugs were orthotopically co-implanted with 4T1 cells into mice in a 1:1 ratio (0.5×10^5 cells) ($n = 5$ mice/group). A schematic representation of the experimental procedure is provided in (A). Tumor growth was assessed regularly until mice from control group reached endpoint (B). Subsequently, tumors and lungs were removed. Tumor sections were stained for lymphatic vessels using anti-LYVE-1 antibodies (red) and nuclei were stained with DAPI (blue). Scale bar, 200 µm (C). Lung sections were stained with H&E and assessed for metastasis. Metastatic lesions per magnified field were counted ($n = 15$ /group). Red arrows point at micrometastases. Scale bar, 200 µm (D). (E) In a parallel experiment, peritoneal macrophages obtained from mice treated with vehicle (Veh), PTX, 31C1, or a combination of the two drugs were orthotopically co-implanted with 4T1 cells into mice in a 1:1 ratio (0.5×10^5 cells) ($n = 8$ mice/group). Mouse survival was monitored, and a Kaplan-Meier survival curve was plotted.

(F) 4T1 cells were orthotopically implanted into the mammary fat pad of BALB/c mice ($n = 6$ mice/group). When tumors reached 350 mm³, mice were injected intraperitoneally with empty liposomes or clodronate-containing liposomes (clodrolip) in order to deplete macrophages. After 3 days, mice were treated with vehicle control, PTX, or PTX and recombinant VEGF-C (50 µg/mouse per day) as described in Experimental Procedures. Tumors were removed 3 days later, and tumor sections were stained for LYVE-1 (red) and DAPI (blue). Scale bar, 200 µm. Error bars indicate SD.

* $p < 0.05$; ** $0.01 \geq p > 0.001$; *** $p \leq 0.001$ (one-way ANOVA followed by Tukey's post hoc test).

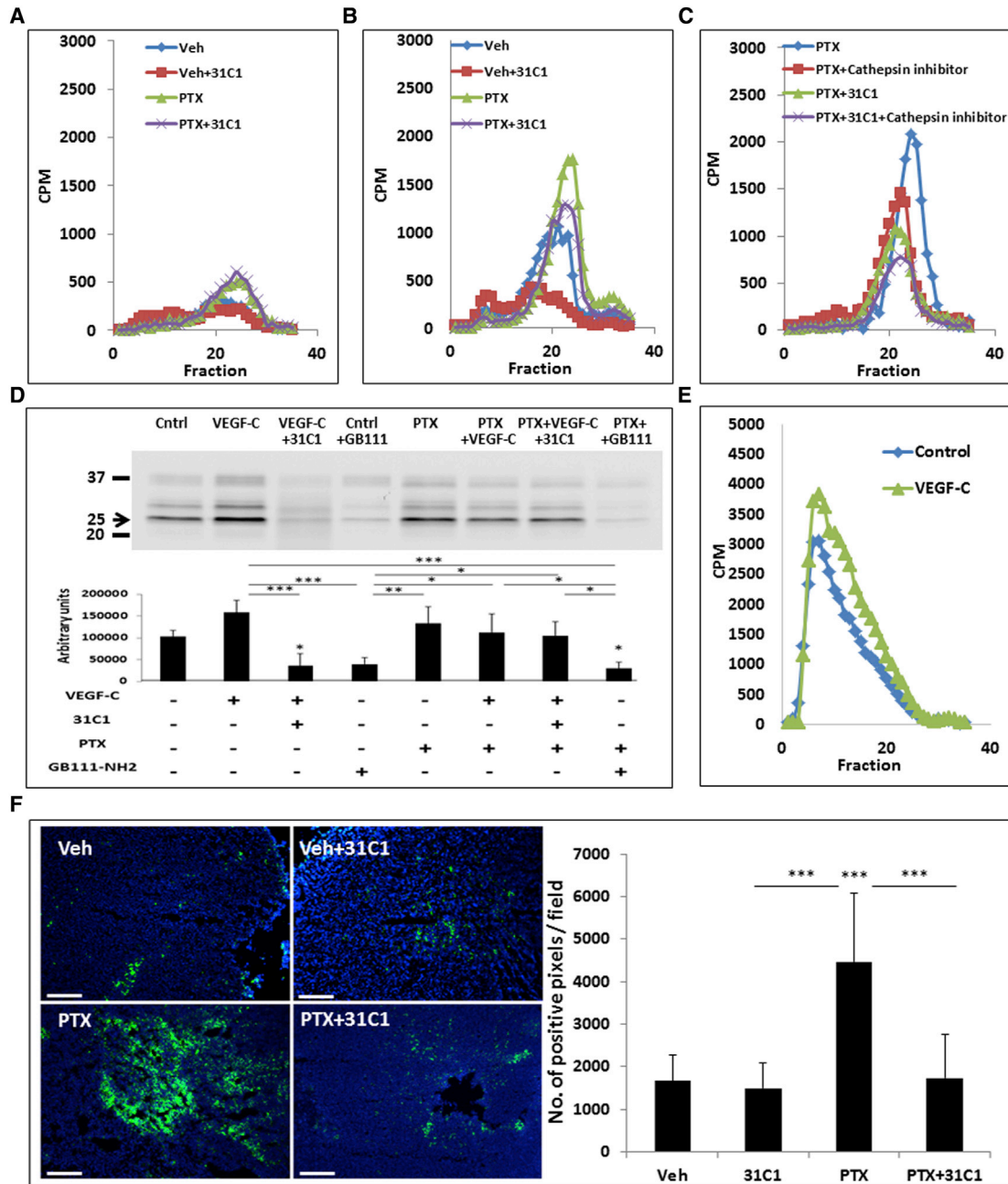


Figure 6. Heparanase and Cathepsin Activity Is Increased in Macrophages from Paclitaxel-Treated Mice in a VEGF-C/VEGFR3-Dependent Manner

(A) Peritoneal macrophages were obtained from mice treated with vehicle (Veh), PTX, 31C1, or a combination of the two drugs (n = 3 mice/group). Conditioned media of the macrophage cultures were collected after 24 hr, adjusted to pH 6.2, and applied to sulfate-labeled ECM dishes. Heparanase enzymatic activity was determined as described in [Experimental Procedures](#).

(B) Conditioned medium of macrophages from treatment groups described in (A) was supplemented with latent heparanase (1 μ g/mL), and heparanase activity was determined as in (A).

(C) Conditioned medium of macrophages from PTX-treated mice (n = 3) supplemented with latent heparanase (1 μ g/mL), 31C1, cathepsin inhibitor, or a combination of the two drugs was applied to sulfate-labeled ECM dishes. Heparanase activity was determined.

(D) Macrophages from control mice or mice treated with PTX in the presence or absence of VEGF-C, cathepsin inhibitor GB111-NH₂, and 31C1 were collected (n = 4 mice/group). Conditioned medium from macrophage cultures was collected and treated with GB123, a fluorescent-activity-based probe. In-gel fluorescence was scanned. The black arrow indicates the fluorescent cathepsin activity band. The experiment was repeated three times. A representative western blot is provided with densitometry analysis of the three biological repeats.

(legend continued on next page)

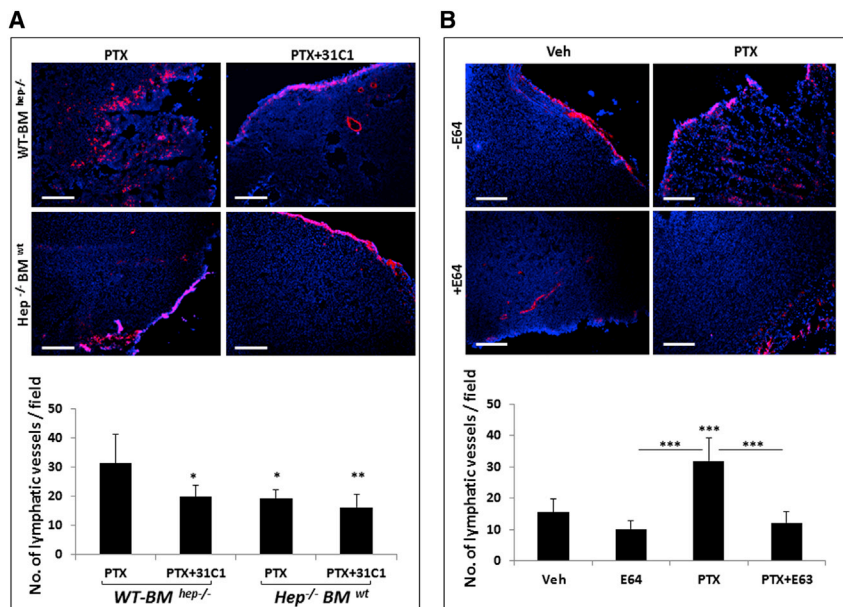


Figure 7. The Lack of Heparanase or Inhibition of Cathepsins in Paclitaxel-Treated Tumors Alters Lymphatic Vessel Phenotype

(A) LLC cells (0.5×10^6) were implanted into the flanks of either chimeric wild-type mice, which were used as recipients of heparanase $-/-$ bone marrow cells (WT-BM^{hep-/-}; $n = 5$ mice/group), or heparanase $-/-$ mice, which were used as recipients of wild-type bone marrow cells (*Hep*^{-/-} BM^{wt}, $n = 5$ mice/group). When tumors reached 500 mm^3 , treatment with PTX or PTX+31C1 was initiated. After 3 days, tumors were removed, and tumor sections were stained for podoplanin (red) and DAPI (blue). Scale bar, $200 \mu\text{m}$. The number of lymphatic vessels per field was counted in tumor sections ($n = 15$ fields/group).

(B) LLC cells (0.5×10^6) were implanted into C57Bl/6 mice ($n = 5$ mice/group). When tumors reached 500 mm^3 , treatment with PTX and/or E64 was initiated according to the schedule and doses described in [Experimental Procedures](#). 3 days later, tumors were removed and sections were immunostained for podoplanin (red) and DAPI (blue). The number of lymphatic vessels per field was counted in tumor sections ($n = 15$ fields/group). Scale bar, $200 \mu\text{m}$. Error bars indicate SD. * $p < 0.05$; ** $0.01 \geq p > 0.001$; *** $p \leq 0.001$ (one-way ANOVA followed by Tukey's post hoc test).

mice treated with PTX, but had little effect on heparanase in conditioned medium of macrophages from mice treated with PTX+31C1 (Figure 6C). Indeed, macrophages cultured with VEGF-C or conditioned medium of macrophages from mice treated with PTX exhibited an elevated level of cathepsin B, an effect that was significantly blocked by 31C1 (Figure 6D). Furthermore, conditioned medium of primary human macrophages cultured in the presence of VEGF-C resulted in increased proteolytic activity, most likely cathepsins, when evaluated for its ability to degrade sulfate-labeled extracellular matrix (ECM) (Bar-Ner et al., 1985) compared to conditioned medium from control macrophages, suggesting that VEGF-C induces protease activity in human macrophages (Figure 6E). In addition, a significant increase in cathepsin B expression was also found in 4T1 tumor sections from mice treated with PTX when compared to mice treated with PTX+31C1 (Figure 6F). These results further suggest that macrophages activate exogenous latent heparanase via cathepsin release, an effect that is most likely regulated by VEGFR3.

Next, to further test whether cathepsin release from macrophages following PTX therapy is primarily regulated by VEGFR3, we performed a bone marrow transplantation experiment in which heparanase $-/-$ mice were transplanted with wild-type BMDCs (*Hep*^{-/-} BM^{wt}) and wild-type mice were transplanted with BMDCs from heparanase $-/-$ mice (WT-BM^{hep-/-}). After

full BMDC reconstitution (Figure S5A), mice were implanted with LLC cells, and when tumors reached 500 mm^3 , treatment with PTX and/or 31C1 was initiated. After 3 days, tumors were resected and tumor sections were stained for lymphatic vessels. The lymphatic vessel phenotype serves as an indication of cathepsin release by BMDCs and subsequent heparanase activation. In this experimental design, WT-BM^{hep-/-} mice lack endogenous heparanase in BMDCs. Therefore, cathepsin release by BMDCs will activate heparanase derived from cells other than BMDCs. In contrast, the *Hep*^{-/-} BM^{wt} mice lack heparanase in all cells other than BMDCs. We found that *Hep*^{-/-} BM^{wt} mice treated with PTX exhibited a lymphatic vessel phenotype similar to that of mice treated with PTX+31C1, as demonstrated by immunostaining with either LYVE-1 or podoplanin; specifically, lymphatic vessels were located at the tumor periphery. However, the lymphatic vessel phenotype in WT-BM^{hep-/-} mice recapitulated the same phenotype observed in wild-type mice; specifically, following PTX therapy the lymphatic vessels were located at the center of the tumor, whereas following treatment with PTX+31C1, the lymphatic vessels were located at the tumor periphery (Figures 7A and S5B). These results indicate that the cleavage of latent heparanase by cathepsins is regulated in part by VEGFR3. Furthermore, plasma VEGF-C levels were assessed 24 hr after non-tumor-bearing heparanase $-/-$ and wild-type mice were treated with PTX.

(E) Human primary macrophages obtained from peripheral blood ($n = 4$), as described in [Experimental Procedures](#), were cultured with or without recombinant VEGF-C ($1 \mu\text{g/mL}$) for 3 days. Conditioned medium was obtained and subsequently supplemented with latent heparanase ($1 \mu\text{g/mL}$). Protease activity (i.e., release of high-molecular-weight materials from sulfate-labeled ECM [fractions 3–15]) was determined (Bar-Ner et al., 1985).

(F) BALB/c mice were orthotopically implanted with 4T1 cells ($n = 5/\text{group}$). When tumors reached a size of 500 mm^3 , treatment with PTX, 31C1, or a combination of the two drugs was initiated. After 3 days, mice were sacrificed, and tumors were sectioned and immunostained for cathepsin B (green). Nuclei were stained with DAPI (blue). Scale bar, $200 \mu\text{m}$. Error bars indicate SD.

* $p < 0.05$; ** $0.01 \geq p > 0.001$; *** $p \leq 0.001$ (one-way ANOVA followed by Tukey's post hoc test).

While levels of plasma VEGF-C were significantly higher in wild-type mice following PTX therapy, in heparanase $-/-$ mice, no significant difference in plasma VEGF-C levels was observed between treated groups (Figure S5C).

We also assessed the contribution of cathepsins to lymphangiogenesis using the cathepsin inhibitor E64. LLC tumors were implanted in C57Bl/6 mice, and when tumors reached 500 mm³, treatment with PTX, E64, or the combination of the two drugs was initiated. After 3 days, tumors were removed, and tumor sections were stained for lymphatic vessels (using either LYVE-1 or podoplanin). The number of lymphatic vessels in mice treated with E64 was dramatically reduced regardless of PTX therapy. Taken together, these results further indicate that cathepsins are major contributors to tumor lymphangiogenesis following PTX therapy, probably via the induction of heparanase activity (Figures 7B and S5D).

DISCUSSION

Breast cancer metastasizes primarily via the lymphatic system and the extent of lymph node involvement is a key prognostic factor (Schoppmann et al., 2004). Upregulation of VEGF-C within tumors in response to various signals leads to the development of a vast lymphatic network, promoting metastatic spread (Alitalo and Carmeliet, 2002; Mandriota et al., 2001; Ni et al., 2013; Skobe et al., 2001). Here, we show that the VEGF-C/VEGFR3 axis is significantly active following PTX chemotherapy among other drugs. PTX increases the levels of circulating VEGF-C in both patients and mouse models, resulting in enhanced lymphangiogenesis. An increased number of lymphatic vessels and their location at the center of the tumor highlight the morphological and biological changes occurring in lymphatic vessels following chemotherapy. LECs exposed to plasma from PTX-treated mice become invasive and migratory, effects that are largely mediated by VEGF-C. As such, the host pro-metastatic effects occurring in response to PTX therapy (Gingis-Velitski et al., 2011) are mediated, at least in part, by VEGF-C.

Macrophages are known to promote tumor angiogenesis, re-growth, and resistance to therapy (Chung et al., 2009; De Palma and Lewis, 2013). It has been shown that macrophages secrete cathepsins in response to PTX therapy, thereby promoting tumor resistance (Shree et al., 2011). Recently, macrophages were shown to reside at the perivascular site and promote tumor revascularization following chemotherapy (Hughes et al., 2015). Macrophages can also induce lymphangiogenesis and thus support tumor metastasis via the lymphatic system (Kim et al., 2009; Shi et al., 2012). We demonstrate that in response to PTX therapy, macrophage activity is regulated by the VEGF-C/VEGFR3 pathway. The number of macrophages in PTX-treated tumors is significantly higher than in vehicle control treated tumors. The initial activation of VEGFR3 in macrophages by systemic VEGF-C overexpression in PTX-treated mice amplifies the expression of VEGF-C in the treated tumor microenvironment and, as a result, increases lymphangiogenesis. Specifically, VEGFR3-expressing macrophages secrete cathepsins that, among other tasks, convert latent heparanase into its active form. Heparanase is an endoglycosidase that cleaves heparan

sulfate (HS) side chains of HS proteoglycans in the ECM and on the cell surface (Arvatz et al., 2011). High levels of active heparanase closely associate with tumor growth and metastasis, in part by inducing lymphangiogenesis (Cohen-Kaplan et al., 2008). Moreover, heparanase levels are elevated in response to anti-cancer treatments (Shafat et al., 2007). In our study, we show that active heparanase is significantly elevated in the conditioned medium of macrophages obtained from mice treated with chemotherapy. Tumor-bearing chimeric mice, whose bone marrow is heparanase deficient, exhibit a lymphatic vessel phenotype following treatment with PTX identical to that observed in tumors from wild-type mice treated with PTX. Furthermore, blocking the VEGFR3 pathway by the addition of 31C1 antibody to PTX inhibits the processing of latent exogenous heparanase. These results suggest that heparanase is a secondary downstream mediator of chemotherapy-induced metastasis via lymphangiogenesis and that these effects are regulated by VEGFR3 expressed on macrophages.

Of particular importance are the findings that tumor cells co-implanted with macrophages obtained from PTX-treated mice exhibit a lymphatic vessel phenotype similar to that of tumors grown in PTX-treated mice. Previous studies indicate that M2 macrophages may account for lymphangiogenesis (Jung et al., 2015; Watari et al., 2014). We have previously shown that following PTX therapy, the balance between M1 and M2 macrophages is disrupted in tumors. The blockade of interleukin 1 β (IL-1 β) in PTX-treated mice results in an increased number of infiltrating M2 macrophages in tumors, leading to increased metastasis (Voloshin et al., 2015). Thus, the specific macrophage state that contributes to tumor lymphangiogenesis following PTX therapy remains to be established. It should be noted that in our co-implantation experiment, the tumors were never exposed to chemotherapy. Thus, these results indicate that the lymphatic vessel phenotype in tumors is mostly mediated by the activity of macrophages in response to therapy. Furthermore, the lymphatic vessel phenotype in tumors co-implanted with macrophages from PTX mice was reversed when compared to co-implantation of tumor cells with macrophages from PTX+31C1-treated mice, further indicating that the effect of lymphatic vessels in tumors is mediated by VEGFR3-expressing macrophages. Moreover, a single dose of anti-VEGFR3 had little effect on lymphangiogenesis in unperturbed tumors, implicating the additional role of VEGFR3 pathways in host cells other than LECs, and thus, the primary effect of blocking the VEGF-C/VEGFR3 axis in activated macrophages following PTX therapy is associated with lymphangiogenesis.

In summary, this study suggests that the blockade of the VEGF-C/VEGFR3 axis reduces the contribution of lymphangiogenesis to metastasis following chemotherapy in two distinct pathways: (1) it directly affects LEC activity in tumors, and (2) it indirectly affects lymphangiogenesis by down-regulating cathepsin release from macrophages, which is otherwise increased in response to chemotherapy. Currently, both VEGFR3 blocking antibodies (IMC-3C5) and heparanase inhibitors (SST0001, M402, PI-88, and PG545) are in various stages of clinical trial evaluation, and their efficacy with or without standard chemotherapy in large patient cohorts is yet to be determined (<http://clinicaltrials.gov>). Based on our results, it would

be of interest to evaluate the clinical outcome of using anti-VEGFR3 antibodies or heparanase inhibitors in combination with chemotherapy in a neoadjuvant treatment setting, when primary tumors are still intact. At this point, the induction of lymphangiogenesis in chemotherapy-treated tumors can be minimized or even negated by blocking VEGFR3 or heparanase, in part by blocking macrophage activity in tumors. This strategy may potentially inhibit metastatic spread.

EXPERIMENTAL PROCEDURES

Cell Lines

Murine LLC, 4T1 murine mammary adenocarcinoma, and A549 human lung carcinoma cell lines were purchased from the American Type Culture Collection (ATCC) and used within 6 months after thawing. LM2-4, a metastatic variant of the MDA-MB-231 human breast carcinoma line (Munoz et al., 2006), was kindly provided by Dr. R.S. Kerbel (Toronto, ON, Canada). LLC cells were grown in DMEM. 4T1, A549, and LM2-4 cells were grown in RPMI-1640 medium. Culture media were supplemented with 10% fetal calf serum, 1% L-glutamine, 1% sodium pyruvate, and 1% streptomycin, penicillin, and neomycin in solution (10 mg/mL; Biological Industries). LECs were purchased from Lonza and cultured on fibronectin-coated plates (10 µg/mL; Biological Industries) with endothelial cell basal medium (EGM; Lonza).

Tumor Models

The use of animals and experimental protocols were approved by the Animal Care and Use Committee of the Technion. 4T1 (5×10^5 cells) and LM2-4 (2×10^6 cells) breast carcinoma cells were implanted orthotopically into the mammary fat pad of 8- to 10-week-old BALB/c and CB.17 SCID female mice, respectively (Harlan). Tumor volume was measured regularly using Vernier calipers according to the formula $\text{width}^2 \times \text{length} \times 0.5$. LLC (5×10^5 cells), and A549 (5×10^6 cells) cells were implanted subcutaneously to the flanks of 8- to 10-week-old C57Bl/6 mice and CB.17 SCID mice, respectively. In some experiments, heparanase $-/-$ and their wild-type counterpart mice (Zcharia et al., 2009) (grown in-house at the Technion) were implanted with LLC cells.

Drugs and Drug Concentrations

PTX (Biolyse Pharma) was injected intraperitoneally at a dose of 25 mg/kg (BALB/c and CB.17 SCID mice) or 50 mg/kg (C57Bl/6 mice) as previously described (Shaked et al., 2008). Vehicle control contained Cremophor EL (527 mg/mL) and 49.7% alcohol (v/v). In some experiments, non-tumor-bearing BALB/c mice were injected with gemcitabine (500 mg/kg), cisplatin (6 mg/kg), and FOLFOX, which is a combination of folinic acid (30 mg/kg), 5-FU (50 mg/kg), and oxaliplatin (14 mg/kg), as previously described (Alishevitz et al., 2014; Shaked et al., 2008). In cell culture, PTX was used at a concentration of 170 ng/mL. Anti-mouse VEGFR3 (31C1), anti-mouse VEGFR2 (DC101), and anti-mouse VEGFR1 (MF1) blocking antibodies (kindly provided by Eli Lilly) were injected intraperitoneally at a dose of 800 µg/mouse as previously described (Hoshida et al., 2006; Laakkonen et al., 2007; Shaked et al., 2005). In some experiments, immunoglobulin rat-IgG antibodies (Jackson ImmunoResearch) were used as an isotype control. Purified VEGF-C protein, generated as described previously (Kirkin et al., 2001), was tested for purity, activity, and endotoxin levels and injected intraperitoneally at a concentration of 50 µg/mouse per day for 3 consecutive days. For in vitro experiments, VEGF-C was added to medium at a concentration of 1 µg/mL. In cell culture, 31C1 antibody was added at a concentration of 10 µg/mL as previously described (Wang et al., 2004). E64 (Sigma-Aldrich), a cathepsin inhibitor, was injected intraperitoneally at a dose of 100 µg/mouse per day before PTX administration for 3 sequential days (Navab et al., 1997).

Bone Marrow Transplantation

Bone marrow transplantation was performed as previously described (Voshin et al., 2015). Details are provided in Supplemental Experimental Procedures.

Flow-Cytometry Acquisition and Analysis

Single-cell suspensions of tumor tissue or peritoneal macrophages were analyzed by flow cytometry in order to evaluate the percentage of LECs, macrophages, and cells expressing VEGFR3. Details are provided in Supplemental Experimental Procedures.

Evaluation of Murine and Human VEGF-C Protein Levels

Blood, BMDCs, organs, and macrophages from murine origin and blood specimens from human origin were evaluated for VEGF-C levels using specific ELISAs. The human study was approved by the ethic committees both at Haemek and at Rambam medical centers, and all patients signed an informed consent. Details are provided in Supplemental Experimental Procedures.

Invasion and Migration Assays

The invasion and migration properties of LECs were assessed using the Boyden chamber assay as previously described (Gingis-Velitski et al., 2011). Details are provided in Supplemental Experimental Procedures.

Tube-Forming Assay

Tube formation of LECs on Matrigel was carried out as previously described (Varshavsky et al., 2008). Details are provided in Supplemental Experimental Procedures.

Immunostaining

Lungs or tumors were embedded in O.C.T. (Sakura) and subsequently frozen at -80°C . Tissue sections (12 µm thick) were prepared using Leica CM 1950 microtome (Leica Microsystems) in order to detect lymphatic vessels, endothelial cells, or metastasis lesions. In some experiments, human tumor specimens were embedded in paraffin, sectioned (6–10 µm thick), and stained for VEGF-C. Details are provided in Supplemental Experimental Procedures.

Macrophage Depletion Using Clodronate Liposomes

For depletion of macrophages, mice were injected intraperitoneally with 200 µL liposomal clodronate (clodrolip) or control liposomes (Macrophage depletion kit, Mannosylated; Encapsula NanoSciences) according to the manufacturer's instructions 72 hr before treatment with PTX and/or 31C1.

Cathepsin and Heparanase Activity Assay

Macrophages obtained from vehicle or PTX-treated BALB/c mice were harvested and cultured in serum-free media. Conditioned medium and cells were evaluated for cathepsin and heparanase activity as described in detail in Supplemental Experimental Procedures.

Statistical Analysis

Data are presented as mean \pm SD. The number of replicates for each experiment is provided in Supplemental Experimental Procedures and/or the figure legends. In the in vitro experiments, an estimate of variance was performed, and parameters for the statistical test were adjusted accordingly. In the in vivo and ex vivo studies, three to eight mice per group (as specified in the figures) were used to reach statistical significance. The sample size for each experiment was designed to have 80% power at a two-sided α of 0.05. To calculate mouse survival, a Kaplan-Meier survival curve statistical analysis was performed in which the uncertainty of the fractional survival of 95% confidence intervals was calculated. A two-tailed Student's t test for a comparison between two groups or one-way ANOVA followed by Tukey's ad hoc statistical test for a comparison between multiple groups was used. For human studies, a paired two-tailed Student's t test was used to make comparisons between baseline and post-therapy. In all experiments, statistical significance was calculated using GraphPad/Prism5. Differences among all groups were compared and considered significant at values below 0.05.

SUPPLEMENTAL INFORMATION

Supplemental Information includes Supplemental Experimental Procedures and five figures and can be found with this article online at <http://dx.doi.org/10.1016/j.celrep.2016.09.083>.

AUTHOR CONTRIBUTIONS

D.A., S.G.-V., Z.V., N.I., D.H., R.S.-F., G.B., J.P.S., I.V., and Y.S. designed experiments. D.A., S.G.-V., L.G.-K., S.D.S., E.M., Y.B.-N., V.M., C.R.-T., M.T., and Z.R. performed experiments. D.A., S.G.-V., O.K.-P., L.G.-K., S.D.S., E.M., Y.B.-N., D.H., Z.Y., N.I., D.L., R.S.-F., G.B., J.P.S., I.V., and Y.S. analyzed data. D.A., O.K.-P., Z.R., D.L., R.S.-F., G.B., J.P.S., I.V., and Y.S. critically reviewed and/or wrote the paper. G.B., J.P.S., I.V., and Y.S. provided funds to support the execution of the experiments. Y.S. supervised the study.

ACKNOWLEDGMENTS

This study was supported by research grants from the European Research Council (under the FP-7 program, 260633), the Israel Science Foundation (490/12), and Israel Cancer Research Funds (708/12) (Y.S.). This study was also supported by research grants from the German Israel Foundation (1204-253.13/2012) (Y.S. and J.P.S.) and the Israeli Society for Clinical Oncology and Radiation Therapy (O.K.-P. and Y.S.).

Received: September 29, 2015

Revised: August 22, 2016

Accepted: September 24, 2016

Published: October 25, 2016

REFERENCES

- Alishekevitz, D., Bril, R., Loven, D., Miller, V., Voloshin, T., Gingis-Velitski, S., Fremder, E., Scherer, S.J., and Shaked, Y. (2014). Differential therapeutic effects of anti-VEGF-A antibody in different tumor models: implications for choosing appropriate tumor models for drug testing. *Mol. Cancer Ther.* **13**, 202–213.
- Alitalo, K., and Carmeliet, P. (2002). Molecular mechanisms of lymphangiogenesis in health and disease. *Cancer Cell* **1**, 219–227.
- Alitalo, A., and Detmar, M. (2012). Interaction of tumor cells and lymphatic vessels in cancer progression. *Oncogene* **31**, 4499–4508.
- Arvat, G., Shafat, I., Levy-Adam, F., Ilan, N., and Vlodavsky, I. (2011). The heparanase system and tumor metastasis: is heparanase the seed and soil? *Cancer Metastasis Rev.* **30**, 253–268.
- Bar-Ner, M., Kramer, M.D., Schirmacher, V., Ishai-Michaeli, R., Fuks, Z., and Vlodavsky, I. (1985). Sequential degradation of heparan sulfate in the subendothelial extracellular matrix by highly metastatic lymphoma cells. *Int. J. Cancer* **35**, 483–491.
- Chung, E.S., Chauhan, S.K., Jin, Y., Nakao, S., Hafezi-Moghadam, A., van Rooijen, N., Zhang, Q., Chen, L., and Dana, R. (2009). Contribution of macrophages to angiogenesis induced by vascular endothelial growth factor receptor-3-specific ligands. *Am. J. Pathol.* **175**, 1984–1992.
- Cohen-Kaplan, V., Naroditsky, I., Zetser, A., Ilan, N., Vlodavsky, I., and Doweck, I. (2008). Heparanase induces VEGF C and facilitates tumor lymphangiogenesis. *Int. J. Cancer* **123**, 2566–2573.
- De Palma, M., and Lewis, C.E. (2013). Macrophage regulation of tumor responses to anticancer therapies. *Cancer Cell* **23**, 277–286.
- Fisher, E.R., Redmond, C., and Fisher, B. (1983). Pathologic findings from the National Surgical Adjuvant Breast Project. VIII. Relationship of chemotherapeutic responsiveness to tumor differentiation. *Cancer* **51**, 181–191.
- Gingis-Velitski, S., Loven, D., Benayoun, L., Munster, M., Bril, R., Voloshin, T., Alishekevitz, D., Bertolini, F., and Shaked, Y. (2011). Host response to short-term, single-agent chemotherapy induces matrix metalloproteinase-9 expression and accelerates metastasis in mice. *Cancer Res.* **71**, 6986–6996.
- Hagemann, T., Biswas, S.K., Lawrence, T., Sica, A., and Lewis, C.E. (2009). Regulation of macrophage function in tumors: the multifaceted role of NF-kappaB. *Blood* **113**, 3139–3146.
- Hoshida, T., Isaka, N., Hagendoorn, J., di Tomaso, E., Chen, Y.L., Pytowski, B., Fukumura, D., Padera, T.P., and Jain, R.K. (2006). Imaging steps of lymphatic metastasis reveals that vascular endothelial growth factor-C increases metastasis by increasing delivery of cancer cells to lymph nodes: therapeutic implications. *Cancer Res.* **66**, 8065–8075.
- Hughes, R., Qian, B.Z., Rowan, C., Muthana, M., Kekikoglou, I., Olson, O.C., Tazzyman, S., Danson, S., Addison, C., Clemons, M., et al. (2015). Perivascular M2 Macrophages Stimulate Tumor Relapse after Chemotherapy. *Cancer Res.* **75**, 3479–3491.
- Jung, J.I., Cho, H.J., Jung, Y.J., Kwon, S.H., Her, S., Choi, S.S., Shin, S.H., Lee, K.W., and Park, J.H. (2015). High-fat diet-induced obesity increases lymphangiogenesis and lymph node metastasis in the B16F10 melanoma allograft model: roles of adipocytes and M2-macrophages. *Int. J. Cancer* **136**, 258–270.
- Kim, K.E., Koh, Y.J., Jeon, B.H., Jang, C., Han, J., Kataru, R.P., Schwendener, R.A., Kim, J.M., and Koh, G.Y. (2009). Role of CD11b+ macrophages in intra-peritoneal lipopolysaccharide-induced aberrant lymphangiogenesis and lymphatic function in the diaphragm. *Am. J. Pathol.* **175**, 1733–1745.
- Kirkin, V., Mazitschek, R., Krishnan, J., Steffen, A., Waltenberger, J., Pepper, M.S., Giannis, A., and Sleeman, J.P. (2001). Characterization of indolinones which preferentially inhibit VEGF-C- and VEGF-D-induced activation of VEGFR-3 rather than VEGFR-2. *Eur. J. Biochem.* **268**, 5530–5540.
- Kukk, E., Lymboussaki, A., Taira, S., Kaipainen, A., Jeltsch, M., Joukov, V., and Alitalo, K. (1996). VEGF-C receptor binding and pattern of expression with VEGFR-3 suggests a role in lymphatic vascular development. *Development* **122**, 3829–3837.
- Laakkonen, P., Waltari, M., Holopainen, T., Takahashi, T., Pytowski, B., Steiner, P., Hicklin, D., Persaud, K., Tonra, J.R., Witte, L., and Alitalo, K. (2007). Vascular endothelial growth factor receptor 3 is involved in tumor angiogenesis and growth. *Cancer Res.* **67**, 593–599.
- Mäkinen, T., Jussila, L., Veikkola, T., Karpanen, T., Kettunen, M.I., Pulkkanen, K.J., Kauppinen, R., Jackson, D.G., Kubo, H., Nishikawa, S., et al. (2001). Inhibition of lymphangiogenesis with resulting lymphedema in transgenic mice expressing soluble VEGF receptor-3. *Nat. Med.* **7**, 199–205.
- Mandriota, S.J., Jussila, L., Jeltsch, M., Compagni, A., Baetens, D., Prevo, R., Banerji, S., Huarte, J., Montesano, R., Jackson, D.G., et al. (2001). Vascular endothelial growth factor-C-mediated lymphangiogenesis promotes tumour metastasis. *EMBO J.* **20**, 672–682.
- Matsumoto, M., Roufail, S., Inder, R., Caesar, C., Karnezis, T., Shayan, R., Farnsworth, R.H., Sato, T., Achen, M.G., Mann, G.B., and Stacker, S.A. (2013). Signaling for lymphangiogenesis via VEGFR-3 is required for the early events of metastasis. *Clin. Exp. Metastasis* **30**, 819–832.
- Munoz, R., Man, S., Shaked, Y., Lee, C.R., Wong, J., Francia, G., and Kerbel, R.S. (2006). Highly efficacious nontoxic preclinical treatment for advanced metastatic breast cancer using combination oral UFT-cyclophosphamide metronomic chemotherapy. *Cancer Res.* **66**, 3386–3391.
- Navab, R., Mort, J.S., and Brodt, P. (1997). Inhibition of carcinoma cell invasion and liver metastases formation by the cysteine proteinase inhibitor E-64. *Clin. Exp. Metastasis* **15**, 121–129.
- Ni, X., Zhao, Y., Ma, J., Xia, T., Liu, X., Ding, Q., Zha, X., and Wang, S. (2013). Hypoxia-induced factor-1 alpha upregulates vascular endothelial growth factor C to promote lymphangiogenesis and angiogenesis in breast cancer patients. *J. Biomed. Res.* **27**, 478–485.
- Schoppmann, S.F., Bayer, G., Aumayr, K., Taucher, S., Geleff, S., Rudas, M., Kubista, E., Hausmaninger, H., Samonigg, H., Gnant, M., et al.; Austrian Breast and Colorectal Cancer Study Group (2004). Prognostic value of lymphangiogenesis and lymphovascular invasion in invasive breast cancer. *Ann. Surg.* **240**, 306–312.
- Shafat, I., Barak, A.B., Postovsky, S., Elhasid, R., Ilan, N., Vlodavsky, I., and Arush, M.W. (2007). Heparanase levels are elevated in the plasma of pediatric cancer patients and correlate with response to anticancer treatment. *Neoplasia* **9**, 909–916.
- Shaked, Y. (2016). Balancing efficacy of and host immune responses to cancer therapy: the yin and yang effects. *Nat. Rev. Clin. Oncol.* **13**, 611–626.
- Shaked, Y., Bertolini, F., Man, S., Rogers, M.S., Cervi, D., Foutz, T., Rawn, K., Voskas, D., Dumont, D.J., Ben-David, Y., et al. (2005). Genetic heterogeneity

- of the vasculogenic phenotype parallels angiogenesis; Implications for cellular surrogate marker analysis of antiangiogenesis. *Cancer Cell* 7, 101–111.
- Shaked, Y., Henke, E., Roodhart, J.M., Mancuso, P., Langenberg, M.H., Coleoni, M., Daenen, L.G., Man, S., Xu, P., Emmenegger, U., et al. (2008). Rapid chemotherapy-induced acute endothelial progenitor cell mobilization: implications for antiangiogenic drugs as chemosensitizing agents. *Cancer Cell* 14, 263–273.
- Shaked, Y., Tang, T., Woloszynek, J., Daenen, L.G., Man, S., Xu, P., Cai, S.R., Arbeit, J.M., Voest, E.E., Chaplin, D.J., et al. (2009). Contribution of granulocyte colony-stimulating factor to the acute mobilization of endothelial precursor cells by vascular disrupting agents. *Cancer Res.* 69, 7524–7528.
- Shi, V.Y., Bao, L., and Chan, L.S. (2012). Inflammation-driven dermal lymphangiogenesis in atopic dermatitis is associated with CD11b+ macrophage recruitment and VEGF-C up-regulation in the IL-4-transgenic mouse model. *Microcirculation* 19, 567–579.
- Shree, T., Olson, O.C., Elie, B.T., Kester, J.C., Garfall, A.L., Simpson, K., Bell-McGuinn, K.M., Zabor, E.C., Brogi, E., and Joyce, J.A. (2011). Macrophages and cathepsin proteases blunt chemotherapeutic response in breast cancer. *Genes Dev.* 25, 2465–2479.
- Skobe, M., Hawighorst, T., Jackson, D.G., Prevo, R., Janes, L., Velasco, P., Riccardi, L., Alitalo, K., Claffey, K., and Detmar, M. (2001). Induction of tumor lymphangiogenesis by VEGF-C promotes breast cancer metastasis. *Nat. Med.* 7, 192–198.
- Sleeman, J.P., and Thiele, W. (2009). Tumor metastasis and the lymphatic vasculature. *Int. J. Cancer* 125, 2747–2756.
- Stacker, S.A., Achen, M.G., Jussila, L., Baldwin, M.E., and Alitalo, K. (2002). Lymphangiogenesis and cancer metastasis. *Nat. Rev. Cancer* 2, 573–583.
- Timaner, M., Bril, R., Kaidar-Person, O., Rachman-Tzemah, C., Alishekevitz, D., Kotsofruk, R., Miller, V., Nevelsky, A., Daniel, S., Raviv, Z., et al. (2015). Dequalinium blocks macrophage-induced metastasis following local radiation. *Oncotarget* 6, 27537–27554.
- Varshavsky, A., Kessler, O., Abramovitch, S., Kigel, B., Zaffryar, S., Akiri, G., and Neufeld, G. (2008). Semaphorin-3B is an angiogenesis inhibitor that is inactivated by furin-like pro-protein convertases. *Cancer Res.* 68, 6922–6931.
- Veikkola, T., Jussila, L., Makinen, T., Karpanen, T., Jeltsch, M., Petrova, T.V., Kubo, H., Thurston, G., McDonald, D.M., Achen, M.G., et al. (2001). Signalling via vascular endothelial growth factor receptor-3 is sufficient for lymphangiogenesis in transgenic mice. *EMBO J.* 20, 1223–1231.
- Voloshin, T., Alishekevitz, D., Kaneti, L., Miller, V., Isakov, E., Kaplanov, I., Voronov, E., Fremder, E., Benhar, M., Machluf, M., et al. (2015). Blocking IL-1beta pathway following paclitaxel chemotherapy slightly inhibits primary tumor growth but promotes spontaneous metastasis. *Mol. Cancer Ther.* 14, 1385–1394.
- Wang, E.S., Teruya-Feldstein, J., Wu, Y., Zhu, Z., Hicklin, D.J., and Moore, M.A. (2004). Targeting autocrine and paracrine VEGF receptor pathways inhibits human lymphoma xenografts in vivo. *Blood* 104, 2893–2902.
- Watari, K., Shibata, T., Kawahara, A., Sata, K., Nabeshima, H., Shinoda, A., Abe, H., Azuma, K., Murakami, Y., Izumi, H., et al. (2014). Tumor-derived interleukin-1 promotes lymphangiogenesis and lymph node metastasis through M2-type macrophages. *PLoS ONE* 9, e99568.
- Welford, A.F., Bizziato, D., Coffelt, S.B., Nucera, S., Fisher, M., Pucci, F., Di Serio, C., Naldini, L., De Palma, M., Tozer, G.M., and Lewis, C.E. (2011). TIE2-expressing macrophages limit the therapeutic efficacy of the vascular-disrupting agent combretastatin A4 phosphate in mice. *J. Clin. Invest.* 121, 1969–1973.
- Zcharia, E., Jia, J., Zhang, X., Baraz, L., Lindahl, U., Peretz, T., Vlodavsky, I., and Li, J.P. (2009). Newly generated heparanase knock-out mice unravel coregulation of heparanase and matrix metalloproteinases. *PLoS ONE* 4, e5181.
- Zhang, Y., Lu, Y., Ma, L., Cao, X., Xiao, J., Chen, J., Jiao, S., Gao, Y., Liu, C., Duan, Z., et al. (2014). Activation of vascular endothelial growth factor receptor-3 in macrophages restrains TLR4-NF- κ B signaling and protects against endotoxin shock. *Immunity* 40, 501–514.